Trans. Indian Inst. Met.
Vol.60, Nos. 2-3, April-June 2007, pp. 103-111

TP 2108

Lead-free Bearing Alloys for Engine Applications Results of the ESA-MAP Project MONOPHAS

L. Ratke[1], S. Brück[1], R. Mathiesen[2], A. Ludwig[3], M. Gruber-Pretzler[3], B. Tonn[4], K. Gzovskyy[4], L. Gránásy[5], G. Tegze[5], J. Agren[6], L. Höglund[6], L. Arnberg[7], E. Gust[8], G. Anger, M. Lauer[10], R. Garen[11] and B. Reifenhäuser[12]

1 Institute of Space Simulation, DLR, D-51147 Cologne, Germany
2 SINTEF, Materials and Technology, N-7465 Trondheim, Norway
3 Department of Metallurgy, University of Leoben, A-8700 Leoben, Austria
4 B. Tonn, Institut of Metallurgy, Technical University Clausthal, D-38678 Clausthal-Zellefeld, Germany
5 Research Institute for Solid State Physics and optics, H-1525 Budapest, Hungary
6 Royal Institut of Technology, Materials Science and Technology, S-10044 Stockholm, Sweden
7 Faculty of Natural Sciences and Technology, NTNU, N-7465 Trondheim, Norway
8 Zollern BHW Gleitlager GmbH, D-38124 Braunschweig, Germany
9 AMAG rolling GmbH, A-5282 Ranshofen, Austria
10 SKF Gleitlager GmbH, D- 66346 Püttlingen, Germany
11 Rolls-Royce Marine AS, N-6065 UlsteinVIK, Norway
12 Federal Mogul, D-65201 Wiesbaden, Germany
E-Mail: lorenz.ratke@dlr.de

(Received 30 June 2006 ; in revised form 20 November 2006)

ABSTRACT

Recent developments to reduce fuel consumption, emission and air pollution, size and weight of engines for automotive, truck, ship propulsion and electrical power generation lead to temperature and load conditions within engines that cannot be provided by conventional bearings. Therefore a European project has been established to develop a technically usable aluminium based lead free bearing material with sufficient hardness, wear and friction properties and good corrosion resistance to be produced with semi-continuous casting process. The paper describes the scientific challenges, approaches to tackle the solidification and casting problems and presents some illustrative research results.

1. INTRODUCTION

Engine bearings are subject to high pulsating load and high surface friction simultaneously. Bearing materials therefore generally consist of a solid solution and/or precipitation hardened non-ferrous matrix in which hard and soft phases are incorporated to provide good tribological properties. The standard bearing material still is of the bronze-lead type having lead contents up to 20 wt.%. The most often used production method is that of direct casting onto a steel support in a continuous way. Generally the bronze-lead type bearings cannot fulfil future requirements concerning for example strength and friction properties. Since the early sixties, materials from the alloy system Al-Sn have been used in the sliding bearing industry [1-3].

Attempts to use materials based on alloys from the systems like Al-Pb, exhibiting a miscibility gap in the liquid state, were made during the last decades with various techniques, since the combination of a hardenable aluminium matrix and soft Pb inclusions with a relatively high melting point always seemed to be the optimum combination for bearing applications [4-11]. All attempts, however, to produce bearings with Al-Pb alloys were failures. The origin was identified as the gravity induced sedimentation of the dense lead phase precipitating during the cooling through the liquid miscibility gap existing in the Al-Pb system.

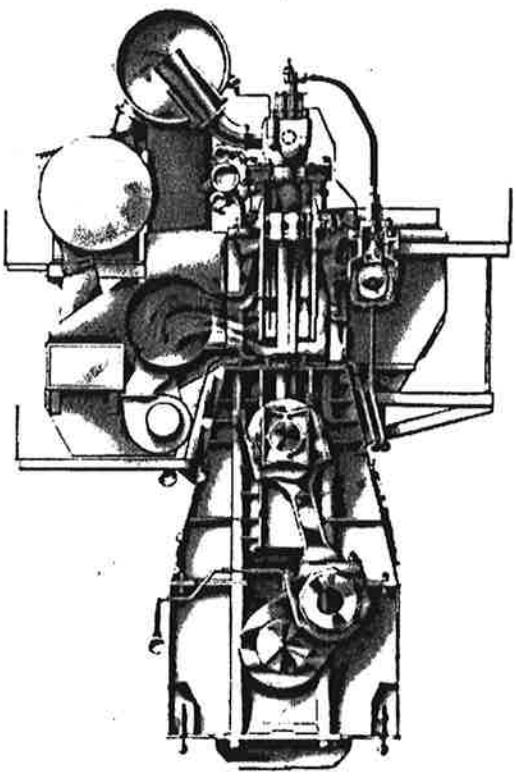

Fig. 1 : Two stroke engine (right) equipped with sliding bearings for the crank and cam shaft, piston bolt and connecting rod (courtesy, Zollern-BHW).

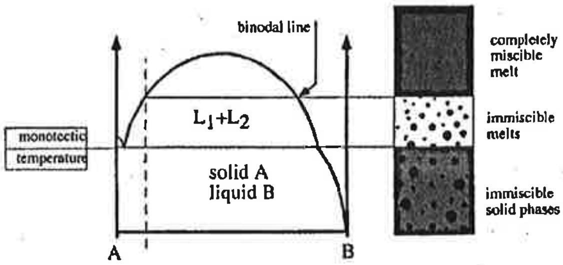

Fig. 2 : Scheme of the solidification of a hypermonotectic alloy passing the miscibility gap.

Recently the difficulties with Al-Pb and similar type immiscible alloys like Al-Bi were solved due to research under reduced gravity conditions pinpointing to the importance of temperature gradient induced motion of Pb droplets during the phase separation process (Marangoni motion) [12-19]. These investigations lead to the development of a new vertical strip casting process (VSCP), which is able to produce two phase microstructures from immiscibles that seem to be suitable for bearings.

The essential scientific challenge today is to control precisely the microstructure evolution during cooling of a multi-component alloy based on the binary Al-Bi. The solidification of alloys being immiscible in the liquid state (see Fig. 2) leads on encounter with the miscibility gap boundary to a liquid-liquid decomposition and spatial microstructure evolution in the molten state prior to the occurrence of a solid phase. Droplets of the minority phase are nucleated below the binodal temperature and grow in the matrix melt. These drops are prone to gravity induced sedimentation due to the fact that the two liquid phases generally have considerable density differences. Interfacial effects also play a prominent role, not only in the absence of gravity (Marangoni motion) [12-19], since they can counteract gravity induced motion. This is of special importance in casting processes utilizing huge temperature gradients like the VSCP. The team of the MONPHAS project therefore attempt to tackle the complex solidification problem by laboratory casting, a pilot-plant casting machine performing VSCP and numerical analysis of the phase separation kinetics on the nanometer scale using phase field methods, process modelling of the VSCP process using multi-phase flow approaches and last but not least the thermodynamics of multi-component Al-Bi-X-Y-Z alloys have to be settled experimentally and theoretically since data are rarely available and needed as inputs for experiments and numerical modelling.

2. EXPERIMENTAL

The alloy in all investigations of the MONOPHAS project is based on the well-known binary Al-Bi. In order to achieve a solid solution strengthening Zn is added. The ternary phase diagram of AlZnBi was recently evaluated experimentally and theoretically by the group of Schmid-Fetzer in Clausthal [20]. The bearing alloy itself contains further alloying elements, Si, Cu, Mn, Fe, Cr, Ti, Sb and others.

2.1 In-situ solidification experiments

The conventional approach to study the phase separation in immiscible alloys is just to cast alloys with different compositions form different cast temperature into different mould materials, just to vary the cooling conditions, the volume fraction of second phase, vary conditions for morphological stability etc. Although this approach has advantages, it has the essential drawback, that the whole sequence from a single phase liquid to a two- or multi-phase solid can not be followed directly but must be reconstructed form metallographic sections after processing. The result might not be unambiguous in the case of immiscible alloys. Therefore a new approach was undertaken by the team at SINTEF to perform experiments in thin slabs allowing to analyse the phase separation and solidification in-situ utilizing synchroton radiation at the ESRF in Grenoble.

The experimental technique has been described in detail elsewhere [21-24]. Binary alloys were prepared by melting high purity Al (99.999 wt.%) and high purity Bi in a fibrefrax coated clay-graphite crucible to obtain a nominal composition of Al-6Bi and a ternary alloy Al-8Zn-6Bi. Directional solidification was undertaken using a Bridgman type furnace and temperatures. The two temperature zones, used to impose the thermal gradient, G, are independently controlled and the temperature gradient varied between 14-60 K/mm. The sample was placed in the hot zone and when completely molten, driven with a constant pulling or pushing velocity, rsp, towards the cold zone. Different sample velocities were used in this series of experiments and varied between 7-36 µm/s. Solidification sequences were undertaken for the Al-6Bi and Al-8Zn-6Bi alloys. It was found that the solidification direction (parallel or anti-parallel) had a significant impact on the Bi particle distribution within the solid Al. Convection was particularly important in the current work (as it strongly affected droplet motion).

Figure 3 shows a solidification sequence from the hypermonotectic Al-6Bi alloy solidified at a pulling speed of ~ 7.2 mm/s and thermal gradient of 14.6 K/mm. In Fig. 3, the size of the Bi droplets (the dark phase) in the solid aluminium appears to have a bimodal distribution. Very fine Bi droplets are inter-dispersed between large round droplets. Ahead of the interface, the liquid phase separation can be seen as Bi droplets of various sizes. They appear to be aligned perpendicular to the interface. During real time observations, the small droplets were observed to move very quickly away from the interface. When the Bi agglomerates reached a critical size (by coagulation), they fell due to gravity and settled on the monotectic interface where they were subsequently engulfed. This is illustrated in Fig. 3 (t=1.5 s to t=2.75 s). Bi droplets (highlighted by the circle) can be observed at t=1.5 s, after t=2.0 s the particles have moved very close to together. At t=2.5 s two larger droplets have formed due to coagulation and begin to settle towards the monotectic interface. This new results clearly indicate that convection at the morphological unstable reaction front is essential for the microstructure evolution and within the convection role the nucleation, growth and especially coagulation of drops determine the drop size distribution in the solid state. The bimodality is well-known and a result of two phase separation processes: the one in the miscibility gap leads to large drops (growth in the liquid, especially by coagulation) and the second one stems from the monotectic reaction itself, leading generally to much finer droplets if the solidification velocity is not too large [25]

2.2 Unidirectional solidification in aerogel mould casting

Laboratory casting using the above mentioned conventional approach allow to scan dozens of alloy compositions and to rapidly check the effect of minor additions on the as-cast

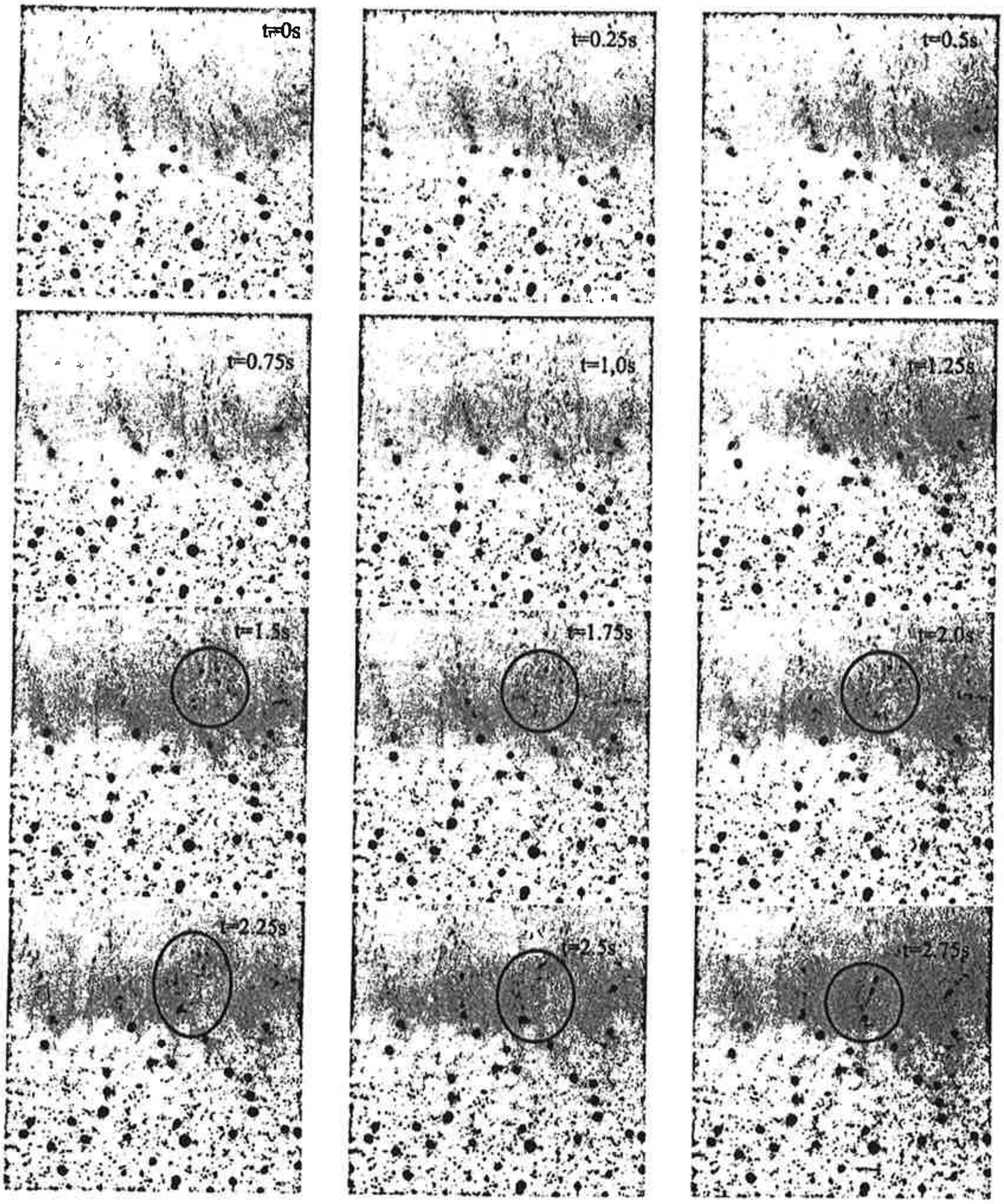

Fig. 3 : Al-6Bi alloy solidified anti-parallel to gravity. The image sizes correspond to a 1.2 x 1.2 mm^2 field of view. The small Bi droplets ahead of the monotectic interface move very rapidly due to convection. When the droplets obtain a critical size, through coagulation, they become to heavy to be supported by convection and fall towards the monotectic interface. Coagulation and settlement of several droplets can be observed from t=1.5 s to t=2.75 s and is highlighted by the circles.

microstructure. This type of investigations are important to develop a multi-component bearing material. Such investigations were performed with AlBi-, AlPb- base alloys in the lab and under microgravity conditions because only there we get an insight into the effect of alloying additions on the Marangioni effect. The AEROCAST device used in microgravity, just recently, is shown in Fig. 4. It uses the periodic variation between low and high-g phases during a parabolic flight of an airplane for casting under 2 g and a controlled directional solidification under microgravity (μg) conditions [15]. During the transition time between hypergravity and microgravity the complete casting facility is turned and the melt being in the hot furnace is cast into an aerogel crucible. The sample material is solidified directionally during the μg-phase. Samples processed with AEROCAST have a cylindrical shape with a length of about 25 to 30 mm and a diameter of 10 mm. typically the solidification speed is 1 mm/s and the temperature gradient vary between 20 K/mm initially to 10 K/mm at the end of

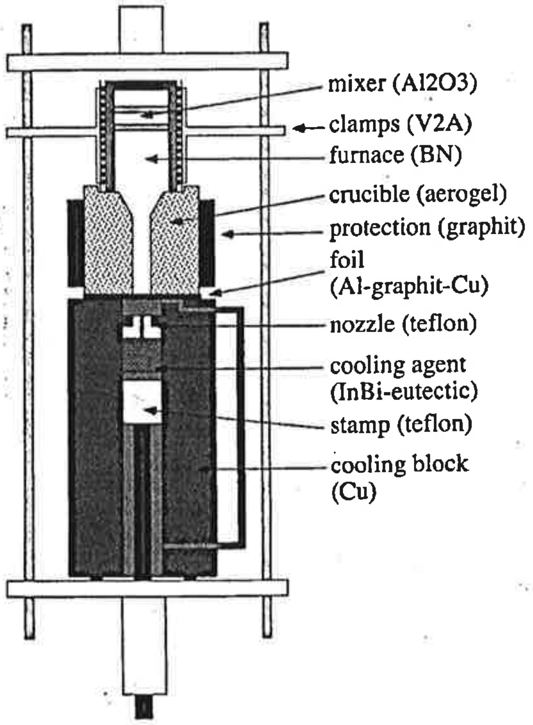

Fig. 4 : Sketch of the AEROCAST device used for casting of immiscibles under microgravity conditions in parabolic flights.

Fig. 5 : AlPb7 under 1g

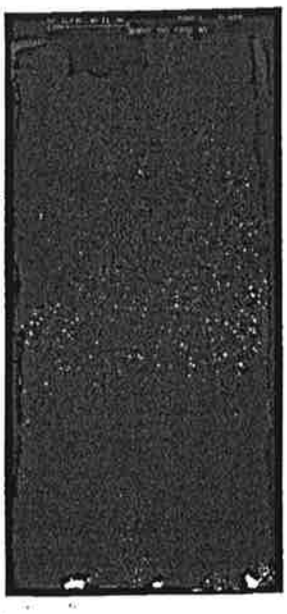

Fig. 6 : AlBi7 under μg

solidification.

The biggest difference between samples processed under reduced gravity conditions and some cast under normal gravity conditions on earth are easily observable and shown in Figs. 5 and 6. Whereas on earth the minority phase droplets are accumulated as big drops or a layer close to the cooling plate the Pb droplets are enriched in the top region of the samples processed under reduced gravity. These results are expected: gravity induced Stokes motion should move the drops such that the immiscible liquids arrange according to their density and Marangoni motion should move the drops from the colder to the hotter region of the samples being always located opposite to the cooling device.

Comparative experiments are performed in the lab with a counter gravity casting device also utilizing aerogels as shown in Fig. 7. Dozens of alloys with different composition from binary to quintinary systems (Al-xBi, Al-xBI-yZn, with x=6,8,10,12 and y=5,6,7,8,9,10 and additions in the range up to 1 wt.% of Ti, Cr, Sb, Mn, Fe, Cu alone or in combinations) were cast. We also used grain refiners (Ti-Boride, -Nitride and -Carbide). The microstructure changes drastically with composition. The alloying elements both influence the liquid-liquid decomposition and the solidification of the primary phase. From the large amount of results the SEM figures microstructures in Fig. 8(a-d) show for example the effects of Cu addition to the Bi precipitation and that adding Sb leads to the formation of a eutectic with a Chinese script like structure. TiB_2 seems to have an effect on the Bi drops: the drops generally become smaller.

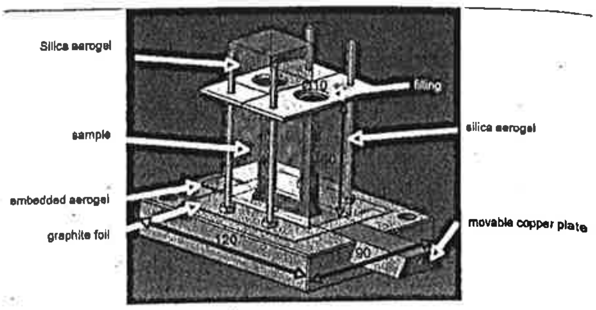

Fig. 7 : Counter gravity casting device

The complete sample sections were analysed with respect to the Bi-droplet size distribution using the Image-Analysis® Software. The size distribution could in most cases be described as a superposition of either two log-normal distributions or as a combination of a power type distribution and a log-normal one. In both cases it was possible to discriminate the droplets stemming form the liquid-liquid decomposition and those originating from the monotectic reaction. This is essential for modelling (see below). The two figures in Fig. 9 show that adding Sb to the ternary AlZnBi alloy gives smaller Bi droplets than the addition of 2 wt.% Cu. The mean of the size distribution differ in both cases by a factor of 1.7. The size distribution of the Bi drops stemming from the monotecti reaction is essentially unaffaected.

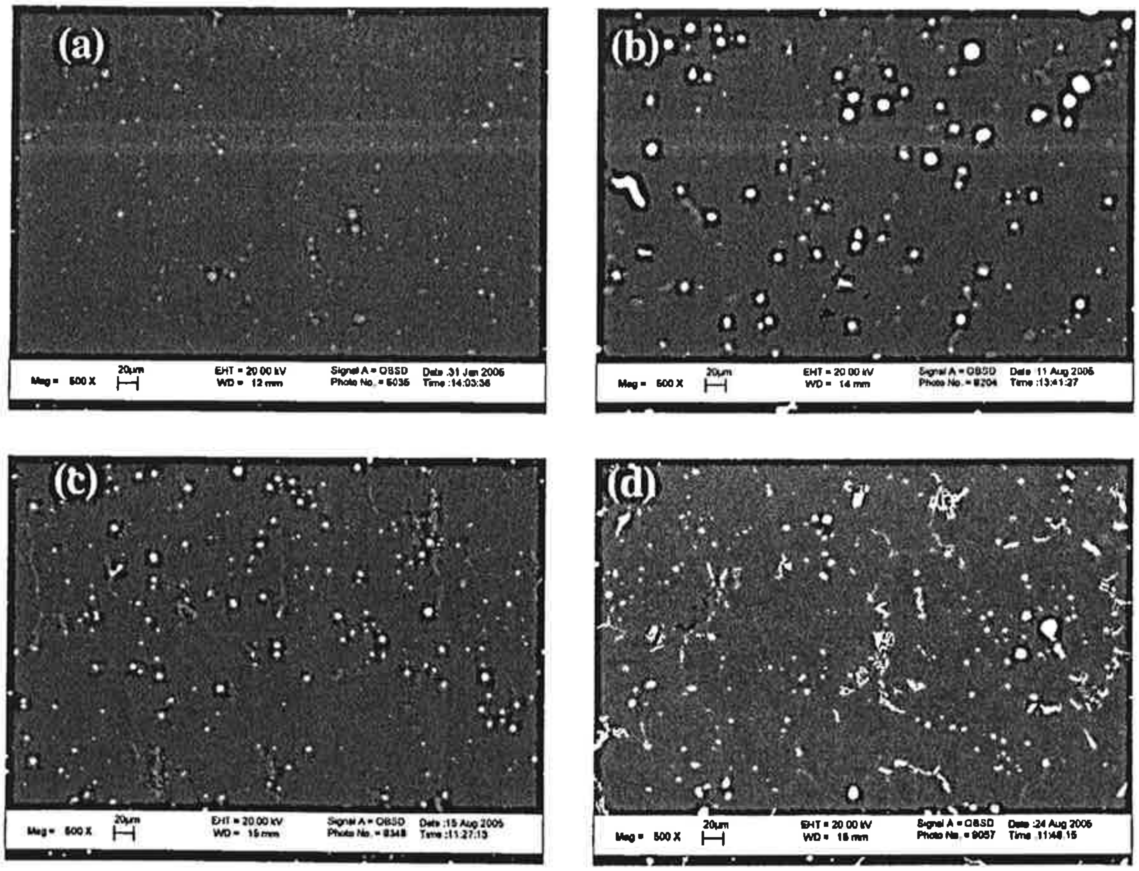

Fig. 8 : (a) AlZn6Bi7, (b) AlZn5Bi8Cu2, (c) AlZn5Bi8Cu2Sb1, (d) AlZn5Bi8Sb1 with TiB

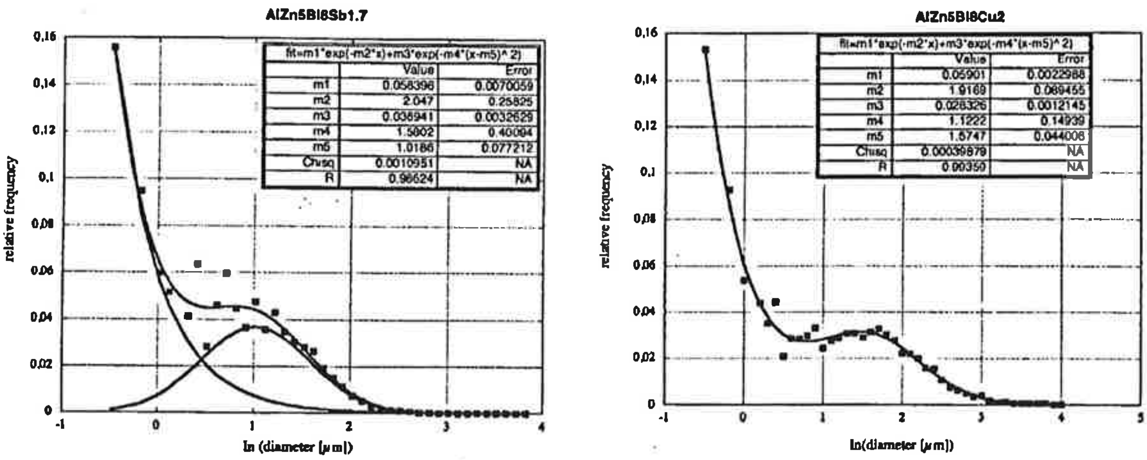

Fig. 9 : Size distributions as measured (dots) and fitted by an overlap of two functions. The drops formed in the miscibility gap are described by a log-normal distribution.

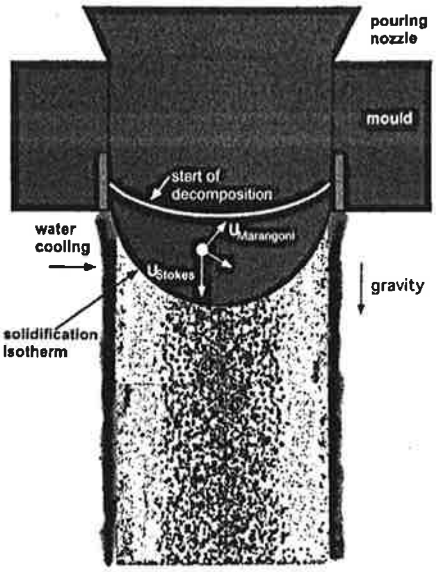

Fig. 10 : Sketch of the Vertical Strip casting Process (VSCP). Strip with a thickness of 10 mm, a width of 10 cm and a length between 1 and 2 m are produced. Casting speed typically is around 50 to 100 cm/minute. In the sketch a micrograph of an AlBiSi alloy is shown. Bi drops are enriched at the strip center 1

2.3. Vertical strip casting

The vertical strip casting machine is routinely operated at the Technical University of Clausthal. It allows to cast strips of 10 mm thickness, 10 cm width and 1 to 2 meters length and was especially developed to cast immiscible alloys. The special problem here is the melt temperature that must be well above the binodal line (and the temperature gradient must be steep in order to produce a sufficiently large Marangoni motion partly counteracting Stopkes motion ahead of the bended solidification isotherm. The large melt temperature of around 1000°C is much higher than typically used for Al-cast alloys. It gives problems in oxidation and additional sensible heat must be removed by the water cooling. A scheme of the VSC process is shown in Fig. 10. The VSC process runs with a solidification velocity of around 10 mm/s and temperature gradients of around 150 K/cm. The plant permits the variation of various process parameters (casting speed, quantity of cooling water, alloy composition, casting temperature), with each affecting the development of the structure in the strip differently. From the dozens of castings performed we show in Fig. 11 one example, which demonstrates the effect of grain refiners. The evaluation of the microstructures with respect to the hypermonotectic particles clearly showed an effect of the two different grain refiners used on the size distribution. This means that heterogeneous nucleation takes place and foreign particles can trigger the liquid-liquid decomposition. This is an essential observation, since it demonstrates that in contrast to earlier experimental and theoretical investigations [19] heterogeneous nucleation of the second liquid phase (here Bi-rich) is possible and that the addition of grain refiners gives an additional lever to influence the as-cast microstructure.

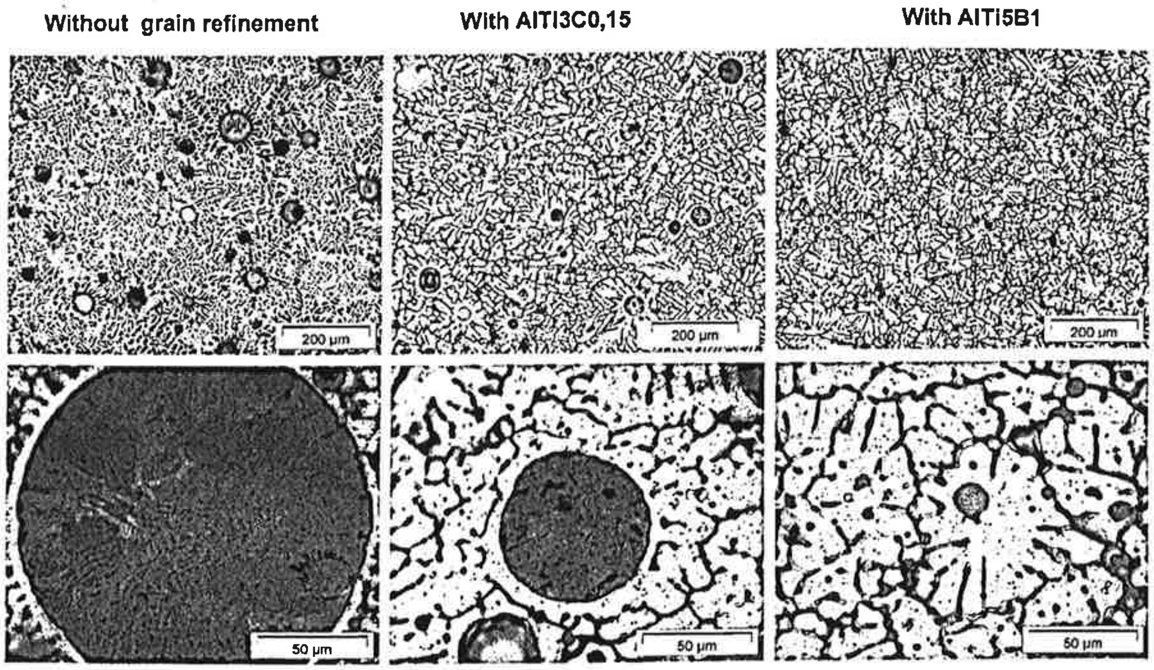

Fig. 11 : Influence of the AlTi5B1 and AlTi3C0,15 Master Alloys on the structure of the AlBi8Zn5Si2, 5Cu alloy. Important is the variation of grain size and it might be interesting to see the crystallization structure inside the large Bi drops. Grain refiners change the Bi drop size and thus it might be concluded that heterogeneous nucleation take place in liquid-liquid decomposition.

3. THEORETICAL DESCRIPTION

3.1. Process modelling

Modelling of the solidification of hypermonotectic alloys belongs to a multiphase problem. An encouraging multiphase volume-averaging (mean field) model was developed by Beckermann's group [26-30] and further modified to study the globular equiaxed solidification by Ludwig et al [31-34]. These previous works laid the foundation for modelling the decomposition and phase separation in hypermonotectic alloys, including both melt convection and droplet motion. The spherical morphology of the decomposed minority phase permits describing the growth kinetics of the droplets more precisely, their hydrodynamic behaviour (drag force), etc. On the other hand, the presence of the minority liquid phase, the gravity induced sedimentation and the Marangoni motion of the minority phase increase the complexity of the model. Therefore, the important tasks of the work for hypermonotectic alloys are to model the decomposition of the minority phase and spatial phase separation including nucleation, droplet growth (coarsening) and dissolution, droplet movement due to gravity sedimentation and Marangoni motion, monotectic reaction and

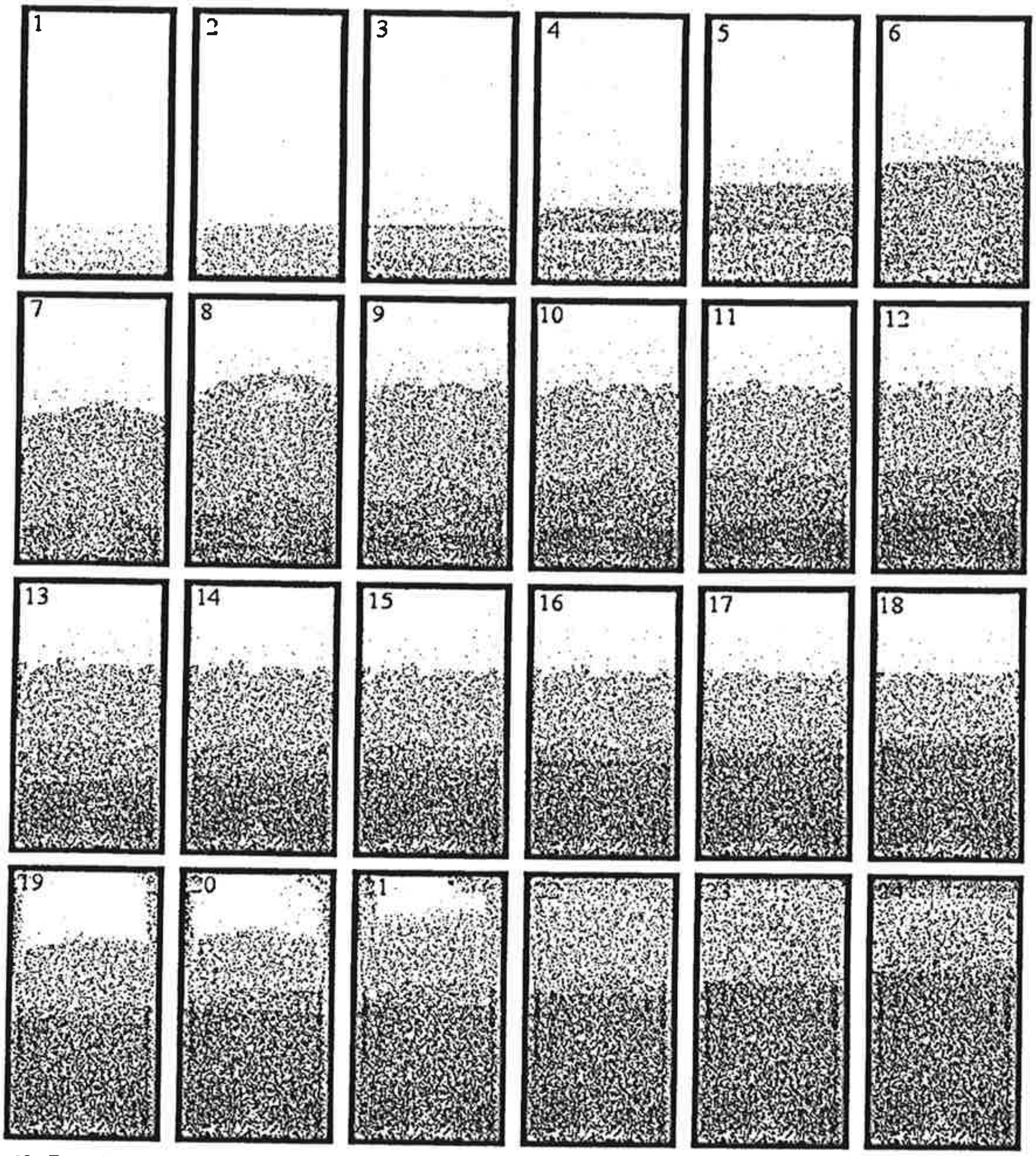

Fig. 12 : Formation of Bi droplets during directional solidification of hypermonotectic Al-Bi. Both the droplet density and the diameter of the droplets, shown in this figure, are reduced and enlarged by corresponding factors so that the droplet distribution can be seen with the naked eye.

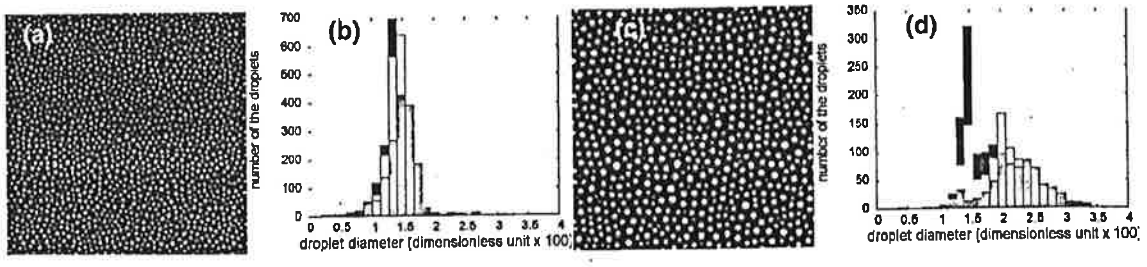

Fig. 13 : Liquid phase separation in Al-Bi as predicted by the phase field theory: (a),(b) Without melt flow and (c),(d) with melt flow. Snapshots of the concentration fields ((a),(c)) taken at dimensionless time 0.051 are shown. Histograms showing the respective droplet size distributions at three dimensionless times (0.025, 0.031, and 0.051) for the two cases are presented in panels (b) and (c).

the final spatial phase distribution. Details for the phase definition and the numerical model itself are systematically described in recent publications [34].

Modelling for instance the directional solidification of AlBi10 alloy in a cylindrical cavity with a constant cooling rate at the top and bottom and isolating walls, thus resembling the counter gravity casting described above or the microgravity experiments in AEROCAST, gives results like those shown in Fig. 12. The overall solidification time is numerically calculated to be 79 s. With 3 s of interval, the decomposition and solidification series from 3 s to 74 s are displayed in the Fig. 12. Nucleation of Bi-droplets starts as soon as the temperature drops below the binodal. Due to the applied cooling conditions, this first happens at the bottom area of the rod. As soon as the Bi-droplets form, they start to submerge and sediment towards the bottom. While the Bi-droplets grow and sink, further nucleation leads to a continuous creation of new Bi-droplets above the already existing ones. The stratifying (layering) of droplets, visible in the first few pictures of Fig. 12, is a result of the limited resolution of the post-processor and do not represent the numerical predictions properly. However, the higher droplet density appearing above the already existing droplets does reveal an improvement of the nucleation conditions caused by the establishment of a stronger temperature gradient and thus higher undercoolings.

The collective downward movement of droplets has to be compensated by an upwards movement of the parent melt. Note that the solidification front is not perfectly flat - a result of the convection-induced perturbations of isotherms and note that this was already seen experimentally in the in-situ x-ray investigations described briefly above. While the solidification front moves from below, the boundary between the droplet-free area and the area filled with droplets has become rather even again. In the meantime, cooling has also started at the top. Therefore, nucleation of Bi-droplets is now also possible at the top of the rod, especially at the top corner regions. The resulting droplets sink downwards along the right and left rod walls (picture 18 and following). This new source of Bi-droplets gets stronger and finally leads to the filling of the remaining areas with droplets. This predicted phase separation phenomenon agrees with experiments performed by Alkemper and Ratke on a chilled cast Al-Bi alloys [12,17].

3.2. Phase field modelling

As clearly demonstrated in the literature hydrodynamic and thermocapillary effects can be essential in the phase separation process of immiscibles droplet, especially to describe the coagulation processes. To account for such effects, the polycrystalline phase field theory developed at RISSPO [35-37] was extended to cover fluid-dynamic effects since now it involves the solution of the Navier-Stokes equation. The model has been adapted to the Al-Bi monotectic system, approximately described thermodynamically by the regular solution model. Representative images on the time evolution of the liquid-liquid phase separation in a temperature gradient are shown in Fig. 13, together with the respective droplet-size distributions as a function of time [38]. In agreement with experiments, we observe Marangoni-motion of the droplets driven by thermocapillary forces. The comparison between the histograms obtained from modelling with and without fluid flow show essential difference known from analytical investigations [39]. The size distribution shown in Fig. 13(b), are strongly skew symmetric to the left and cut off at larger sizes, whereas the distributions in Fig. 13(d) are more symmetric and have larger particles at the same time. This is in full agreement with diffusional growth of the Bi droplets. In such a case the smaller drops grow faster than larger ones and thus the size distribution must be skew symmetric [39]. Coagulation on the other hand is largest between drops of different size. Marangoni motion induced convecto-diffusive mass transport would change the size distribution to be symmetric around the average and second coagulations rapidly lead to larger sizes and make the distribution at greater times skew symmetric to the right. Thus the phase field model used describes very well what was anticipated from simplified analytical models, but without using such simplifications.

The models developed so far describe binary systems. In order to deal at least with ternary systems they will be extended in the future. The thermodynamic database for AlZnBi is already assessed and is multi-component variants in the Al-rich corner are being investigated.

4. CONCLUSION

The combined approach experiments and theory in the project gives a good chance that the project will have developed at the end at least the basics for the production of advanced lead free bearings in engine applications.

ACKNOWLEDGEMENTS

The authors gratefully acknowledge the financial support from ESA-MAP programme under contract number AO-99-026-15004/01/NL/SH.

REFERENCES

1. Forrester P G, *Metal Industry*, (1962) 185.
2. Hodes E, Aluminiumlegierungen als Werkstoffe für Gleitlager (II), *Aluminium*, **56** (1980) 332.
3. Dobiejewski Z, *Schmierungstechnik*, **18** (1987) 205.
4. Clarke A B and Gregg H H, Patent GB **132 984** (1919).
5. Michael A D and Pratt G C, Patent DE **1 533 254** (1969).
6. Pathak, J P, Tiwari S N and Malhorta S L, Technolgy **11** (1979) 442.
7. Ichikawa K and Ishizuka S, *J. Jap. Inst. Metals* **49** (1985) 1093.
8. Howe D P, Torrance A A and Williams J D, *Mater. Sci. Technol.* **7** (1991) 330.
9. Mohan S, Agarwala V and Ray S, *Mater. Trans. JIM* **33** (1992) 1057.
10. Mohan S, Agarwala V and Ray S, *Mater. Trans. JIM* **33** (1992) 860.
11. Mohan S, Agarwala V and Ray S, *Mater. Sci. Eng.* **A144** (1991), 215.
12. Alkemper J and Ratke L, *Z. Metallkde.* **85**, (1994) 365.
13. Andrews B, *Immiscible Liquid Metals and Organics*, edited by Ratke L, DGM-Informationsgesellschaft, Oberursel, (1993) 199.
14. Diefenbach S, Ph.D. thesis, Ruhr-Universität Bochum (1994).
15. Ratke L and Korekt G, *Z. Metallkd.* **91** (2000) 919.
16. Ratke L, Drees S, Diefenbach S, Prinz B and Ahlborn H, *Materials and Fluids under Low Gravity*, edited by Ratke L, Walter H, Feuerbacher B, Lecture Notes in Physics, Springer Verlag, Berlin, **464** (1996) 115.
17. Alkemper J and Ratke L, *Adv. Colloid Interface Sci.*, **58** (1995) 151.
18. Prinz, B, Romero A and Ratke L, *J. Mater. Sci.* **30** (1995) 4715.
19. Ratke L and Diefenbach S, *Mater. Sci. Eng. Rep.* **R15** (1995) 263.
20. Gröbner J, Mirkoviæ D and Schmid-Fetzer R, *Acta Mater.*, **53** (2005) 3271.
21. Mathiesen R H, Arnberg L, Mo F, Weitkamp T and Snigirev A, *Phys. Rev. Lett.* **83** (1999) 5062.
22. Mathiesen R H, Arnberg L, Mo F, Weitkamp T and Snigirev A, *ESRF Higlights*, (1999) 78.
23. Mathiesen R H, Arnberg L, Ramsøskar K, Weitkamp T, Rau C and Snigirev A, *Metall. Mater. Trans.* **B33** (2002) 613
24. Mathiesen R H and Arnberg L, *Proc. Modelling of Casting Welding and Advanced Solidification Processes – X (MCWASP-X)*. Stefanescu D M, Warren J A, Jolly M R, and Krane M J M, eds. TMS, Warrensdale, PA, (2003) 677
25. Schmidt-Hohagen F, Ratke L, Zhao J and He J, *Trans. Ind. Inst. Metals*, **60** (2007) 303.
26. Beckermann C and Viskanta R, *Appl. Mech. Rev*, **46** (1993) 1.
27. Ni J and Beckermann C, *Metall. Trans.*, **22B** (1991) 349.
28. Wang C Y and Beckermann C, *Metall. Mater. Trans.*, **27A** (1996) 2754.
29. Wang C Y and Beckermann C, *Metall. Mater. Trans.*, **27A** (1996) 2765.
30. Wang C Y and Beckermann C, *Metall. Mater. Trans.*, **27A** (1996) 2784.
31. Ludwig A and Wu M. *Metall. Mater. Trans.*, **33** (2002) 3673.
32. Ludwig A and Wu M. *Adv. Eng. Mater*, **5** (2003) 62.
33. Ludwig A and Wu M, Bührig-Polaczek A, Fehlbier M, Sahm P R. *Inter. J. Heat Mass Transfer*, **46** (2003) 2819.
34. Wu M, Ludwig A and Ratke L, *Modell. Simu. Mater. Sci. Eng.* **11** (2003) 755.
35. Gránásy L, Pusztai T, Tóth G, Jurek Z, Conti M and Kvamme B, *J. Chem. Phys.* **119** (2003) 10376.
36. Gránásy L, Börzsönyi T, Pusztai T, *J. Cryst. Growth* **237-239** (2002) 1813.
37. Gránásy L, Börzsönyi T and Pusztai T, *Phase field theory of nucleation and growth in binary alloys*. Interface and Transport Dynamics, Computational Modelling, edited by Emmerich H, Nestler B and Schreckenberg M, Lecture Notes in Computational Science and Engineering,, Springer, Berlin, **32** (2003) 190.
38. Tegze G and Gránásy L, *Proc. of Modeling of Casting, Welding and Advanced Solidification Processes* - XI, eds. Ch.-A. Gandin, Bellet M, (TMS), Warrendale, (2006) 513.
39. Ratke L and Voorhees P W, Growth and Coarsening, Springer, Berlin (2002).